processes

MDPI

Article

Estimating Relaxation Time and Fractionality Order Parameters in Fractional Non-Fourier Heat Conduction Using Conjugate Gradient Inverse Approach in Single and Three-Layer Skin Tissues

Piran Goudarzi [1], Awatef Abidi [2,3,4], Seyed Abdollah Mansouri Mehryan [5,*], Mohammad Ghalambaz [6,7] and Mikhail A. Sheremet [8,*]

1 Department of Mechanical Engineering, Shahrood University of Technology, Shahrood 3619995161, Iran; pirangoodarzi@yahoo.com
2 Physics Department, College of Sciences Abha, King Khalid University, Abha City 61421, Saudi Arabia; abidiawatef@yahoo.fr
3 Research Laboratory of Metrology and Energy Systems, National Engineering School, Energy Engineering Department, Monastir University, Monastir City 5000, Tunisia
4 Higher School of Sciences and Technology of Hammam Sousse, Sousse University, Sousse City 4011, Tunisia
5 Young Researchers and Elite Club, Yasooj Branch, Islamic Azad University, Yasooj 7591493686, Iran
6 Metamaterials for Mechanical, Biomechanical and Multiphysical Applications Research Group, Ton Duc Thang University, Ho Chi Minh City 758307, Vietnam; mohammad.ghalambaz@tdtu.edu.vn
7 Faculty of Applied Sciences, Ton Duc Thang University, Ho Chi Minh City 758307, Vietnam
8 Laboratory on Convective Heat and Mass Transfer, Tomsk State University, 634050 Tomsk, Russia
* Correspondence: alal1713662244@gmail.com (S.A.M.M.); sheremet@math.tsu.ru (M.A.S.)

check for updates

Citation: Goudarzi, P.; Abidi, A.; Mehryan, S.A.M.; Ghalambaz, M.; Sheremet, M.A. Estimating Relaxation Time and Fractionality Order Parameters in Fractional Non-Fourier Heat Conduction Using Conjugate Gradient Inverse Approach in Single and Three-Layer Skin Tissues. *Processes* **2021**, *9*, 1877. https://doi.org/10.3390/pr9111877

Academic Editor: Yo-Ping Huang

Received: 24 August 2021
Accepted: 19 October 2021
Published: 21 October 2021

Abstract: In this work, the relaxation parameter (τ) and fractionality order (α) in the fractional single phase lag (FSPL) non-Fourier heat conduction model are estimated by employing the conjugate gradient inverse method (CGIM). Two different physics of skin tissue are chosen as the studied cases; single and three-layer skin tissues. Single-layer skin is exposed to laser radiation having the constant heat flux of Q_{in}. However, a heat pulse with constant temperature is imposed on the three-layer skin. The required inputs for the inverse problem in the fractional diffusion equation are chosen from the outcomes of the dual phase lag (DPL) theory. The governing equations are solved numerically by utilizing implicit approaches. The results of this study showed the efficiency of the CGIM to estimate the unknown parameters in the FSPL model. In fact, obtained numerical results of the CGIM are in excellent compatibility with the FSPL model.

Keywords: inverse fractional non-Fourier; fractional heat conduction; parameter estimations; tissues

1. Introduction

Inverse analysis has received more attention recently due to its wide applications in engineering and industry. Inverse problems are often used in engineering problems where direct measurements are difficult in the body. An inverse problem in heat transfer is important and includes obtaining surface temperature, diffuse heat flux, heat source, conductivity and displacement coefficients, and so on. The available literature shows the use of inverse analysis in the non-Fourier heat conduction problem is novel. The unknown or non-measurable parameters in the problems can be estimated using inverse analysis methods such as the conjugate gradients method with/without adjoint problem and the Levenberg–Marquardt algorithm.

The dual-phase-lag (DPL) non-Fourier technique base on the Levenberg–Marquardt non-linear parameter estimation (LMNPE) approach is utilized to predict the thermal diffusivity and the time lags at the presence of a pulse heating [1]. Hsu and Chu [2] studied a non-Fourier heat conduction electronic device to obtain the temperature of

the surface. They used the linear least-squares method to obtain the solution. Yang [3] estimated boundary conditions in the 2D field of hyperbolic heat conduction problems. The modified Newton–Raphson technique is employed for the inverse analysis and it is observed that this method leads to simpler expressions compared to the non-linear least-squares technique. Hsu [4] provided a linear least-squares inverse technique to estimate the unknown temperature on the boundary in a 3D non-Fourier heat conduction problem. Moreover, various types of heat transfer Fourier [5,6] and non-Fourier [7,8] and bioheat transfer [9–11] problems have been investigated in the literature.

Liu and Lin [12] obtained the phase lag times of tissue by employing the DPL model, utilizing the experimental input. In this work, a hybrid scheme of the least-squares technique, change of variables for a direct problem, and Laplace transform are applied. They also investigated the impact of measurement locality on the computed results. Azimi et al. [13] employed the ACGM in an inverse non-Fourier heat transfer problem to compute the root temperature of a fin having diverse profiles. They used the function-estimation form of ACGM, utilizing the border temperature evaluation. They found that ACGM can be used to analyze the non-Fourier inverse heat transfer of fins in various conditions.

Das et al. [14] estimated the coefficients of extinction and conduction-radiation by minimizing the objective function in a non-Fourier conduction-radiation heat transfer problem. The genetic algorithm (GA) is used for this purpose. Ghazizadeh et al. [15] estimated the relaxation time and fractionality order in the fractional single-phase lag (FSPL) heat model for two different physics. The LMNPE method is used to solve the inverse FSPL heat conduction. Their results illustrated that the LMNPE technique can be successfully used to solve the problem of inverse fractional heat transfer. Azimi et al. [16] estimated root temperature distribution in several fins having non-Fourier behavior. This study considered the function-estimation form of the ACGM applying boundary temperature valuations to solve the inverse problem. The results showed that the ACGM method can be recognized as a stable and reliable method for determining temperature boundary conditions in the non-Fourier problems.

Wu et al. [17] employed a conjugate gradient inverse method (CGIM) to estimate the unknown boundary pulse heat flux in a limitless-length cylinder. They solved the problem with the hyperbolic heat conduction and DPL heat transfer theory. Mozafarifard et al. [18] employed FSPL and DPL techniques to investigate transient non-Fourier heat transfer in an upstanding expanded surface with an energy source at the presence of a periodic temperature imposed on the expanded surface root. This study, for the first time, used LMNPE to obtain the heat flux relaxation time and fractional derivation orders for an upstanding fin with the mentioned conditions.

Ali et al. [19] used an inverse method to determine the time-dependent source term for the space-time fractional differential equation based on Caputo derivative in two problems. They investigated the stability and well pose of the inverse problem. Cheng et al. [20] obtained the space-dependent source term in the time-fractional diffusion equation based on Caputo derivative. They used the CGM method to solve the inverse problem. Their results show the effectiveness of the CGM method to obtain unknown functions. Sun and Liu [21] applied the CGM method to obtain a time-dependent source in the time-fractional diffusion equation. Their results were validated by several numerical examples. Tuan et al. [22] determined an unknown source term for fractional diffusion equation based on the Riemann-Liouville derivative. They employed the quasi-boundary value approach to arrange the unstable inverse problem. Their results show convergence of the method.

In the present research, for the first time, the CGIM algorithm is utilized to estimate the undetermined parameters of τ and α of the fractional non-Fourier model in two different physics of skin tissues with single or three-layer tissues. The single-layer tissue is affected by laser radiation having the constant energy of Q_{in}. However, three-layer skin tissue is heated by a source having a constant temperature. These two physics with different conditions were studied by Goudarzi and Azimi [23] to develop the capability of FSPL. The

relaxation and fractionality order parameters in a try and error manner are investigated to capture FSPL results by employing DPL parameters as inputs.

2. Conjugate Gradient Inverse Method

The CGIM is a powerful iterative technique for solving linear and nonlinear inverse problems of parameter estimation. In the iterative procedure of the CGIM, at each iteration, appropriate step size is chosen along a descanting direction to minimize the objective function [24]. Herein, the fractionality order, i.e., α, and the relaxation parameter, i.e., τ, in the FSPL model are unknown. This inverse problem is solved by utilizing the measured outcomes of the case studies presented in [25,26]. This method minimizes the least-squares norm of the evaluated temperatures resulted from DPL, i.e., θ_{DPL}, and FSPL, i.e., θ_C, as expressed below [24]:

$$S(P) = [\theta_C(P) - \theta_{DPL}][\theta_C(P) - \theta_{DPL}]^{Tr} \tag{1}$$

where $P^{Tr} = [\tau\ ,\ \alpha]$. In the current work, an alternative technique is used for the estimation of unknown parameters in the CGIM based on [20]. The CGIM algorithm can be found in [24] in detail. By initial guess for unknown parameters, i.e., α_0 and τ_0, the iteration process starts. Then, the governing equations are solved and follow the iterative procedure until the stopping criterion. The stopping criterion is as follows:

$$\left| P^{m+1} - P^m \right| < \varepsilon \tag{2}$$

where ε is a suitable tolerance and m is the iterations number. It is worth mentioning that the discretized equations are implemented using FORTRAN programming language. The governing equations of each case study are separately given below.

3. Governing Equations and Discretization

In this research, two different cases are studied. One is related to single-layer skin tissue and the other one is for three-layer tissue. As previously discussed, these cases were investigated by Goudarzi and Azimi [23]. They used the numerical FSPL method to simulate non-Fourier heat conduction in the skin tissue to calculate undetermined the parameters by try and error approach. In the present research, inverse analysis based on the conjugate gradient method is used.

3.1. Test Case 1

3.1.1. Direct Problem

Figure 1 depicts a schematic view of the single-layer skin. The thickness, i.e., h, and initial temperature, i.e., θ_0, of the skin are 1 mm and 37 °C, respectively. When $t = 0^+$, laser radiation having an energy of Q_{in} is radiated on the left side of the domain for 5 s, then it is stopped. The governing equation of this case is as the following [23]:

$$\frac{\partial q}{\partial t} + {\tau_q}^{\alpha} \frac{\partial^{1+\alpha} q}{\partial t^{1+\alpha}} = D\, \frac{\partial^2 q}{\partial x^2} + D w_b \rho_b c_b \frac{\partial \theta}{\partial x} \tag{3}$$

The controlling boundary conditions can be defined as the following:

$$\begin{array}{ll} \forall\ x,\ t |\ x = 0, & 0 < t < 5\ s \Rightarrow q = Q_{in}(1 - R_d) \\ \forall\ x,\ t |\ x = h, & 0 < t < 40\ s \Rightarrow q = 0 \end{array} \tag{4}$$

The initial conditions are as follows:

$$\forall\ x,\ t |\ 0 < x < h,\ \ t = 0 \Rightarrow q(x) = 0, \quad \frac{\partial q}{\partial t} = 0 \tag{5}$$

The controlling equation of temperature field is:

$$\rho c \frac{\partial \theta}{\partial t} = -\frac{\partial q}{\partial x} + w_b \rho_b c_b (\theta_b - \theta) + q_{met} + q_{ext} \tag{6}$$

The discretization of the governing equations and the numerical method can be found in [23]. In Figure 1 one can find the following parameters, like P is a general node, E and W are its neighboring nodes to the east and west. The east and west sides of the control volume are identified as e and w. Δx and h are the size of control volume and the thickness of the skin tissue, respectively.

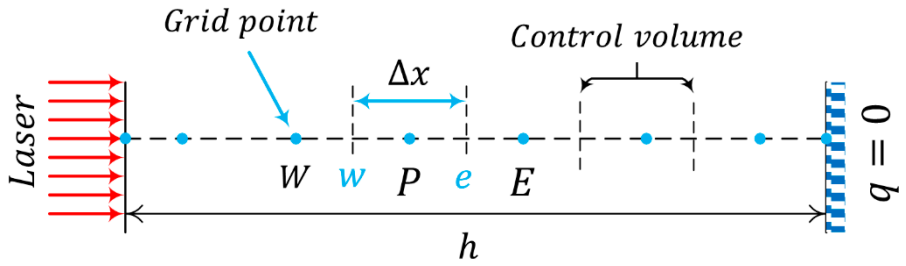

Figure 1. A schematic view of the physical model.

3.1.2. Inverse Problem

The conjugate gradient parameter estimation method is used to evaluate the undetermined parameters in the FSPL model, described in Section 2 in detail. There are two undefined parameters, namely τ and α. Hence, two sensitivity equations along with the initial and boundary conditions are needed to be solved: one is for τ and the other one is for α. To obtain the sensitivity equation for τ, Equations (3)–(5) should be derived with respect to τ.

$$\frac{\partial}{\partial \tau}\left(\frac{\partial q}{\partial t}\right) + \frac{\partial}{\partial \tau}\left(\tau_q{}^{\alpha} \frac{\partial^{1+\alpha} q}{\partial t^{1+\alpha}}\right) = \frac{\partial}{\partial \tau}\left(D \frac{\partial^2 q}{\partial x^2}\right) + \frac{\partial}{\partial \tau}\left(D w_b \rho_b c_b \frac{\partial \theta}{\partial x}\right) \tag{7}$$

$$\frac{\partial}{\partial \tau}\left(\rho c \frac{\partial T}{\partial t}\right) = \frac{\partial}{\partial \tau}\left(-\frac{\partial q}{\partial x}\right) + \frac{\partial}{\partial \tau}(w_b \rho_b c_b (\theta_b - \theta)) + \frac{\partial q_{met}}{\partial \tau} + \frac{\partial q_{ext}}{\partial \tau} \tag{8}$$

with the following boundary conditions:

$$\begin{array}{l} \forall\, x,\, t |\, x = 0,\, 0 < t < 5s \Rightarrow \frac{\partial q}{\partial \tau} = \frac{\partial}{\partial \tau}(Q_{in}(1 - R_d)) \\ \forall\, x,\, t |\, x = h,\, 0 < t < 40s \Rightarrow \frac{\partial q}{\partial \tau} = 0 \end{array} \tag{9}$$

The initial condition is

$$\forall\, x,\, t |\, 0 < x < h,\ \ t = 0 \Rightarrow \frac{\partial \theta(x)}{\partial \tau} = \frac{\partial \theta_b}{\partial \tau} = 0, \qquad \frac{\partial q}{\partial \tau} = 0, \quad \frac{\partial}{\partial \tau}\left(\frac{\partial q}{\partial t}\right) = 0 \tag{10}$$

As presented in Appendix A, the sensitivity coefficients equation of the relaxation time is expressed as the following:

$$\begin{array}{l} \frac{\partial J_{q\tau}}{\partial t} + \tau_q{}^{\alpha} \frac{\partial^{1+\alpha} J_{q\tau}}{\partial t^{1+\alpha}} = D \frac{\partial^2 J_{q\tau}}{\partial x^2} + D\, w_b \rho_b c_b \frac{\partial J_\tau}{\partial x} - \alpha\, \tau_q{}^{\alpha-1} \frac{\partial^{1+\alpha} q}{\partial t^{1+\alpha}} \\ \rho c \frac{\partial J_\tau}{\partial t} = -\frac{\partial J_{q\tau}}{\partial x} - w_b \rho_b c_b J_\tau \end{array} \tag{11}$$

with the following boundary conditions:

$$\begin{array}{l} \forall\, x,\, t |\, x = 0,\, 0 < t < 5s \Rightarrow J_{q_\tau} = 0 \\ \forall\, x,\, t |\, x = h,\, 0 < t < 40s \Rightarrow J_{q_\tau} = 0 \end{array} \tag{12}$$

Initial condition is:

$$\forall\, x,\ t|\ 0 < x < h,\ \ t = 0 \Rightarrow\ J_\tau\ = 0, \qquad J_{q_\tau} = 0, \qquad \frac{\partial J_{q_\tau}}{\partial t} = 0 \tag{13}$$

where J_{q_τ} and J_τ are the heat flux and temperature sensitivities with respect to τ, respectively. Transferring Equations (3)–(5) to α space leads to the following equations:

$$\frac{\partial}{\partial \alpha}\left(\frac{\partial q}{\partial t}\right) + \frac{\partial}{\partial \alpha}\left({\tau_q}^{\alpha}\frac{\partial^{1+\alpha} q}{\partial t^{1+\alpha}}\right) = \frac{\partial}{\partial \alpha}\left(D\,\frac{\partial^2 q}{\partial x^2}\right) + \frac{\partial}{\partial \alpha}\left(D\mathrm{w}_b\rho_b c_b\frac{\partial \theta}{\partial x}\right) \tag{14}$$

$$\frac{\partial}{\partial \alpha}\left(\rho c\frac{\partial \theta}{\partial t}\right) = \frac{\partial}{\partial \alpha}\left(-\frac{\partial q}{\partial x}\right) + \frac{\partial}{\partial \alpha}(\mathrm{w}_b\rho_b c_b(\theta_b - \theta)) + \frac{\partial q_{met}}{\partial \alpha} + \frac{\partial q_{ext}}{\partial \alpha} \tag{15}$$

According to the Appendix A, the sensitivity coefficients equations of fractionality order can be obtained as:

$$\begin{array}{l} \frac{\partial J_{q_\alpha}}{\partial t} + {\tau_q}^{\alpha}\frac{\partial}{\partial \alpha}\left(\frac{\partial^{1+\alpha} q}{\partial t^{1+\alpha}}\right) = D\frac{\partial^2 J_{q_\alpha}}{\partial x^2} + D\ \mathrm{w}_b\rho_b c_b\frac{\partial J_\alpha}{\partial x} - {\tau_q}^{\alpha}\ \ln(\tau)\frac{\partial^{1+\alpha} q}{\partial t^{1+\alpha}} \\ \frac{\partial J_\alpha}{\partial t} = -\frac{\partial J_{q_\alpha}}{\partial x}\ + D\ \mathrm{w}_b\rho_b c_b(\theta_b - J_\alpha) \end{array} \tag{16}$$

with the boundary and initial conditions expressed below:

$$\begin{array}{l} \forall\, x,\ t|\ x = 0,\ 0 < t < 5s \Rightarrow J_{q_\alpha} = 0 \\ \forall\, x,\ t|\ x = h,\ 0 < t < 40s \Rightarrow J_{q_\alpha} = 0 \\ \forall\, x,\ t|\ 0 < x < h,\ \ t = 0 \Rightarrow\ J_\alpha\ = 0, \qquad J_{q_\alpha} =\ 0, \qquad \frac{\partial J_{q_\alpha}}{\partial t} = 0 \end{array} \tag{17}$$

where J_{q_α} and J_α are the heat flux and temperature sensitivities with respect to α, respectively. The finite volume method is employed to discretize Equations (11)–(13), (16), and (17) as presented in Appendix B. Then, the tridiagonal matrix algorithm is applied to solve the algebraic form of controlling equations.

3.2. Test Case 2

3.2.1. Direct Problem

Initially, the skin is exposed to a heat pulse with a constant temperature of 100 °C for 15 s. The heat flux applied to the skin can be resulted from immediate contact with the hot water. After heating, cooling the skin surface is done by a water-ice mixture of 0 °C for 30 s. Figure 2 depicts a schematic view of physics.

The governing equations can be formulated as follows:

$$\begin{array}{l} \frac{\partial \theta}{\partial t} + {\tau_q}^{\alpha}\frac{\partial^{1+\alpha}\theta}{\partial t^{1+\alpha}} + \frac{\mathrm{w}_b\rho_b c_b}{\rho_i c_i}{\tau_q}^{\alpha}\frac{\partial^{\alpha}\theta}{\partial t^{\alpha}} = D_i\frac{\partial^2\theta}{\partial x^2} + \frac{\mathrm{w}_b\rho_b c_b}{\rho_i c_i}(\theta_b - \theta) \\ \qquad + \frac{q_{ext}+q_{met}}{\rho_i c_i} + \frac{{\tau_q}^{\alpha}}{\rho_i c_i}\frac{\partial^{\alpha}}{\partial t^{\alpha}}(q_{ext} + q_{met}) + \frac{{\tau_q}^{\alpha}}{\rho_i c_i}\frac{\partial^{\alpha}}{\partial t^{\alpha}}(\mathrm{w}_b\rho_b c_b\theta_b) \end{array} \tag{18}$$

Here i is the number of layers.

The boundary conditions are as follows:

$$\begin{array}{l} \forall\, x,\ t|\ x{=}\ 0, 0 < t \le 45 \Rightarrow \theta(t) = 100(1 - u(t - 15)) \\ \forall\, x,\ t|\ x = h, 0 < t \Rightarrow \theta(t) = \theta_b =\ 37\ ^\circ\mathrm{C} \end{array} \tag{19}$$

Moreover, the initial conditions are as the following:

$$\forall\, x,\ t|\ 0 < x < h,\ \ t = 0 \Rightarrow \theta(x) = \theta_b =\ 37\ ^\circ\mathrm{C}, \qquad \frac{\partial\theta(x)}{\partial t} = \frac{\partial^2\theta(x)}{\partial t^2} = 0 \tag{20}$$

The discretization of the governing equations and the utilized numerical method are discussed in [23] in detail.

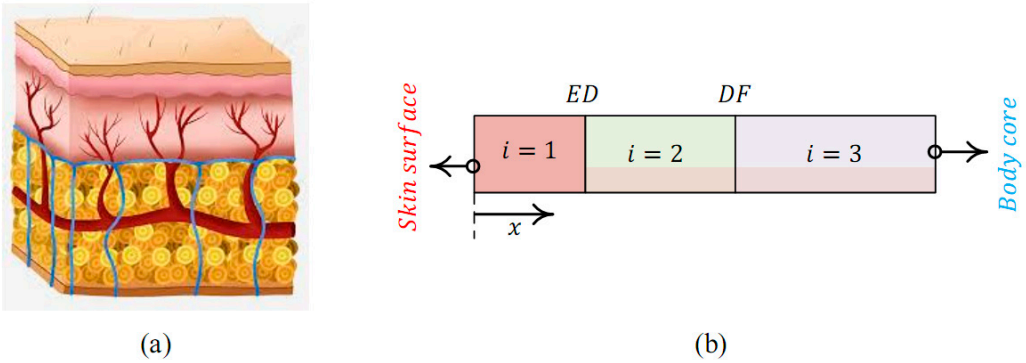

Figure 2. (**a**) Schematic view of the skin tissue, and (**b**) tissue layers; i = 1 for epidermis, i = 2 for dermis, and i = 3 for subcutaneous fat.

3.2.2. Inverse Problem

Similar to the previous one, for using the conjugate gradient method, two sensitivity equations should be obtained with their initial and boundary conditions: one is for τ and the other one is for α. Equations (18)–(20) can be derived with respect to τ as the following:

$$\frac{\partial}{\partial \tau}\left(\frac{\partial \theta}{\partial t}+{\tau_q}^{\alpha}\frac{\partial^{1+\alpha}\theta}{\partial t^{1+\alpha}}+\frac{w_b\rho_b c_b}{\rho_i c_i}{\tau_q}^{\alpha}\frac{\partial^{\alpha}\theta}{\partial t^{\alpha}}\right)=\frac{\partial}{\partial \tau}\left(D_i\frac{\partial^2\theta}{\partial x^2}+\frac{w_b\rho_b c_b}{\rho_i c_i}(\theta_b-\theta)+\frac{q_{ext}+q_{met}}{\rho_i c_i}\right) \tag{21}$$

with the boundary and initial conditions:

$$\begin{array}{l}\forall\, x,\, t|\; x=0, 0<t\le 45\,, \quad \frac{\partial\theta(t)}{\partial\tau}=\frac{\partial}{\partial\tau}(100-100u(t-15))\\ \forall\, x,\, t|\; x=h, 0<t\,, \; \frac{\partial\theta(h,t)}{\partial\tau}=\frac{\partial\theta_b}{\partial\tau}\\ \forall\, x,\, t|\; 0<x<h, t=0\,, \; \frac{\partial\theta(x)}{\partial\tau}=\frac{\partial\theta_b}{\partial\tau} \quad \text{and} \quad \frac{\partial}{\partial\tau}\left(\frac{\partial\theta(x)}{\partial t}\right)=\frac{\partial}{\partial\tau}\left(\frac{\partial^2\theta(x)}{\partial t^2}\right)=0\end{array} \tag{22}$$

The equation expressed below is the sensitivity coefficients equation of the relaxation time:

$$\frac{\partial J_\tau}{\partial t}+{\tau_q}^{\alpha}\frac{\partial^{1+\alpha}J_\tau}{\partial t^{1+\alpha}}+\frac{w_b\rho_b c_b}{\rho_i c_i}{\tau_q}^{\alpha}\frac{\partial^{\alpha}J_\tau}{\partial t^{\alpha}}=D_i\frac{\partial^2 J_\tau}{\partial x^2}-\frac{w_b\rho_b c_b}{\rho_i c_i}J_\tau-\alpha{\tau_q}^{\alpha-1}\frac{\partial^{1+\alpha}\theta}{\partial t^{1+\alpha}} \tag{23}$$

with the initial and boundary conditions expressed below:

$$\begin{array}{l}\forall\, x,\, t|\; 0<t<45,\; t=0\Rightarrow J_\tau(x)=0 \quad \text{and} \quad \frac{\partial J_\tau(x)}{\partial t}=\frac{\partial^2 J_\tau(x)}{\partial t^2}=0\\ \forall\, x,\, t|\; x=0,\; 0<t<45\Rightarrow J_\tau=0\\ \forall\, x,\, t|\; x=h,\; 0<t\Rightarrow J_\tau=0\end{array} \tag{24}$$

where J_τ is the temperature sensitivity to τ.

The sensitivity equations of the layers for α can be obtained by transferring Equations (18)–(20) to the α space:

$$\frac{\partial}{\partial \alpha}\left(\frac{\partial \theta}{\partial t}+{\tau_q}^{\alpha}\frac{\partial^{1+\alpha}\theta}{\partial t^{1+\alpha}}+\frac{w_b\rho_b c_b}{\rho_i c_i}{\tau_q}^{\alpha}\frac{\partial^{\alpha}\theta}{\partial t^{\alpha}}\right)=\frac{\partial}{\partial \alpha}\left(D_i\frac{\partial^2\theta}{\partial x^2}+\frac{w_b\rho_b c_b}{\rho_i c_i}(\theta_b-\theta)+\frac{q_r+q_m}{\rho_i c_i}\right) \tag{25}$$

The controlling boundary and initial conditions are:

$$\begin{array}{l}\forall\, x,\, t|\; x=0, 0<t\le 45\,, \quad \frac{\partial\theta(t)}{\partial\alpha}=100\frac{\partial}{\partial\alpha}(1-u(t-15))\\ \forall\, x,\, t|\; x=h, 0<t\,, \; \frac{\partial\theta(h,t)}{\partial\alpha}=\frac{\partial\theta_b}{\partial\alpha}\\ \forall\, x,\, t|\; 0<x<h, t=0\,, \; \frac{\partial\theta(x)}{\partial\alpha}=\frac{\partial\theta_b}{\partial\alpha} \quad \text{and} \quad \frac{\partial}{\partial\alpha}\left(\frac{\partial\theta(x)}{\partial t}\right)=\frac{\partial}{\partial\alpha}\left(\frac{\partial^2\theta(x)}{\partial t^2}\right)=0\end{array} \tag{26}$$

As shown in Appendix A, the sensitivity coefficients equation for the fractionality order, i.e., α, is expressed below.

$$\begin{gathered}\frac{\partial J_\alpha}{\partial t}+\tau_q{}^\alpha\frac{\partial^{1+\alpha}J_\alpha}{\partial t^{1+\alpha}}+\frac{w_b\rho_bc_b}{\rho_ic_i}\tau_q{}^\alpha\frac{\partial^\alpha J_\alpha}{\partial t^\alpha}=D_i\frac{\partial^2J_\alpha}{\partial x^2}-\frac{w_b\rho_bc_b}{\rho_ic_i}J_\alpha-\tau_q{}^\alpha\ln\tau\frac{\partial^{1+\alpha}\theta}{\partial t^{1+\alpha}}\\ -\tau_q{}^\alpha\frac{\partial\sigma_{1+\alpha}}{\partial\alpha}\sum_{j=1}^{n}w_j^{1+\alpha}\left(\theta_i^{n-j+1}-2\theta_i^{n-j}+\theta_i^{n-j-1}\right)-\tau_q{}^\alpha\sigma_{1+\alpha}\sum_{j=1}^{n}\frac{\partial w_j^{1+\alpha}}{\partial\alpha}\left(\theta_i^{n-j+1}-2\theta_i^{n-j}+\theta_i^{n-j-1}\right)\end{gathered}\tag{27}$$

The initial and boundary conditions in the α space are defined as the following:

$$\begin{gathered}\forall\ x,\ t|\ 0<x\le h,\ t=0\Rightarrow J_\alpha(x)=0\quad\text{and}\quad\frac{\partial J_\alpha(x)}{\partial t}=\frac{\partial^2J_\alpha(x)}{\partial t^2}=0\\ \forall\ x,\ t|\ x=0,\ 0<t\le45\Rightarrow J_\alpha=0\\ \forall\ x,\ t|\ x=h,\ 0<t\Rightarrow J_\alpha=0\end{gathered}\tag{28}$$

From the above equations, J_α is the sensitivity equation to α. The tridiagonal matrix algorithm is utilized to solve the governing algebraic system of equations resulting from the finite difference method. It is worth noting that the values of relevant parameters used in the present work are for real skin tissue as presented in [25].

4. Results and Discussion

In this section, the calculated numerical results, including the time lag and fractionality order in the FSPL non-Fourier model are presented. In both cases, the initial values of α and τ are accidentally chosen. Then, the direct and inverse problems, as well as the sensitive equations, are solved by using the inverse conjugate method introduced above. The solution process continues to iterate until satisfying the convergence criteria according to Equation (2). The tolerance in the stopping criterion, i.e., $\varepsilon = 10^{-4}$, is considered for both cases in Equation (2).

4.1. Test Case 1

For test case 1, the initial guesses of $\alpha_0 = 0.9$ and $\tau_0 = 10$ are used. The direct problem with Equations (3)–(6), and the sensitivity problem with Equations (11)–(13), (16), and (17) are solved and the convergence occurs after 38 iterations. The time-lag and fractionality as two unknown parameters are obtained as the follows:

$$\tau = 16\text{ s},\ \alpha = 0.9985068$$

Figure 3 depicts the temperature history on the skin surface obtained by conjugate gradient parameter estimation inverse analysis. As shown, the CGIM in the estimation of unknown parameters in the non-Fourier heat conduction fractional single-phase lag model is accurate and reliable. Figure 4 illustrates the Jacobian coefficient of the order of fractionality and the relaxation time. To obtain the correct estimation, the Jacobian coefficients should not be linearly related to each other. As can be seen in Figure 4, there is no linear dependence between Jacobian coefficients.

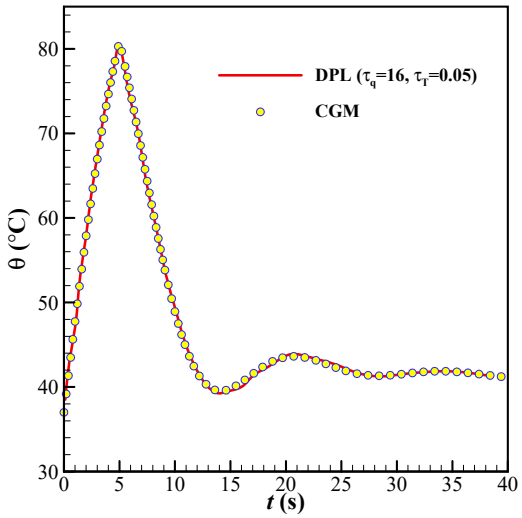

Figure 3. Comparison of the estimation temperature history from the FSPL model with the measured temperature from the DPL model for test case 1.

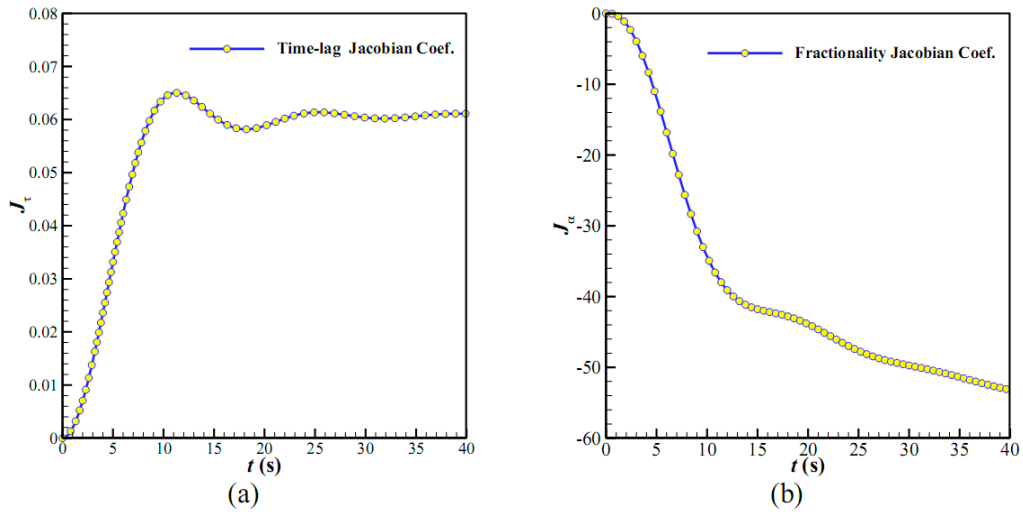

Figure 4. Jacobian coefficient for test case 1; (**a**) time-lag Jacobian coefficient and (**b**) fractionality Jacobian coefficient.

4.2. Test Case 2

Herein, the initial guesses are α_0 = 0.9 and τ_0 = 15. The direct problem with the governing Equations (18)–(20), and the sensitivity problem with Equations (23)–(28) are solved and the convergence occurs after 52 iterations. The two unknown parameters are estimated as the following:

$$\tau = 9.888 \text{ s}, \alpha = 0.986$$

The temperature history resulted from conjugate gradient parameter estimation inverse analysis is depicted in Figure 5. Figure 6 shows the Jacobian coefficient of the fractionality order and the relaxation time. As can be observed, the Jacobian coefficients are non-zero and non-linearly related to each other. Therefore, the required conditions for obtaining the unknown parameters are provided. Once again, the accuracy of the CGIM for estimating unknown parameters in the non-Fourier heat conduction FSPL model is proved. For other values of temperature phase lag in the DPL method, the CGIM is utilized to determine the fractionality and time-lag as the unknown parameters. The results are tabulated in Table 1. As τ_T tends to zero, the fractionality, i.e., α, approaches one. This means that the fractional non-Fourier model is approaching the single phase non-Fourier

thermal wave model. It is also observed that an increment in τ_q leads to increasing time-lag, meaning an increase in non-Fourier effects.

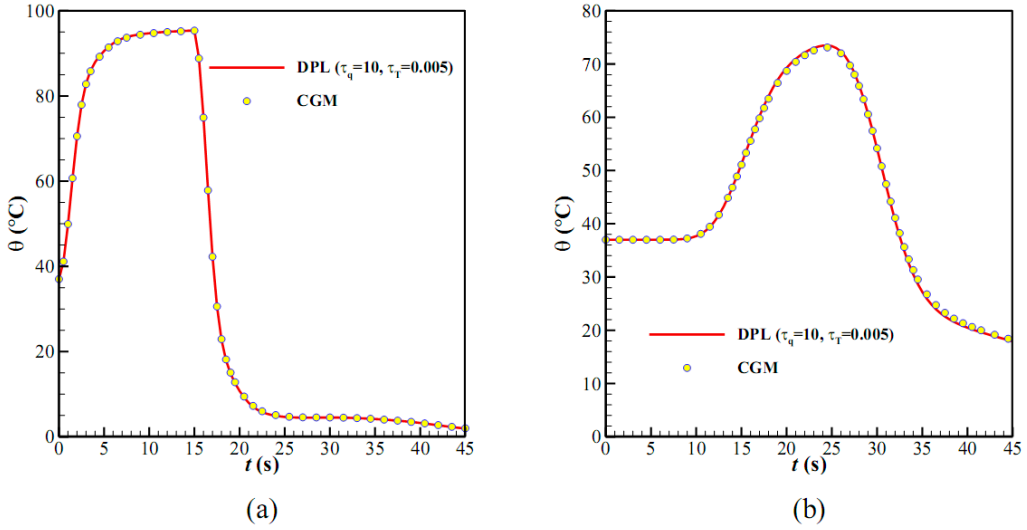

Figure 5. Comparison of the estimation temperature history from the FSPL model with the measured temperature from the DPL model for test case 2 (**a**) at the ED interface and (**b**) at the DF interface in skin tissue.

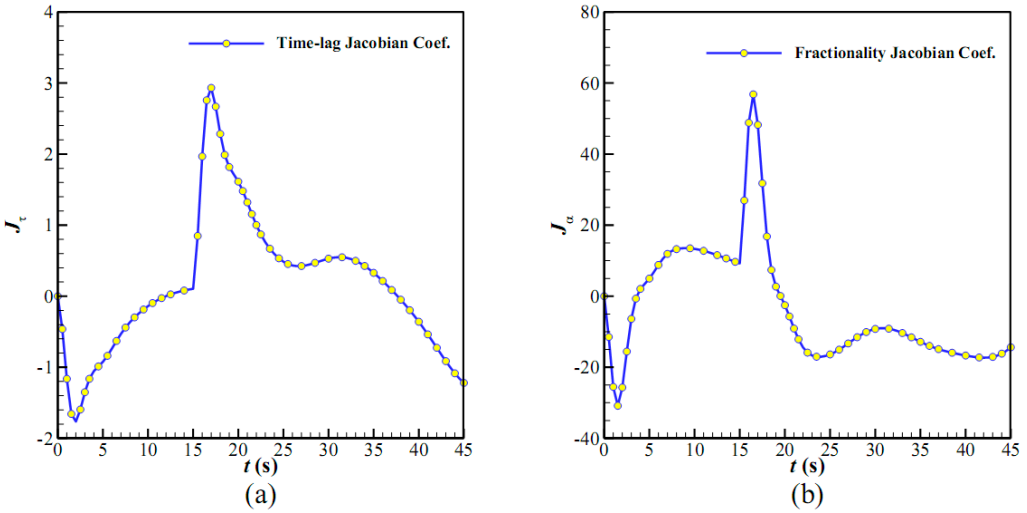

Figure 6. Jacobian coefficient for test case 2 (**a**) time-lag Jacobian coefficient and (**b**) fractionality Jacobian coefficient.

Table 1. Estimation values of fractionality and time-lag in the conjugate gradient method in three samples for test case 2.

	CGIM		DPL	
	α	τ	τ_T	τ_q
Sample A	0.985707860045904	9.88794652835751	0.005	10
Sample B	0.982593197834287	9.82287275801926	0.05	10
Sample C	0.958513945252591	9.87599109128811	0.1	10
Sample D	0.933915800219504	0.57923029381419	0.05	1
Sample E	0.982593197834287	9.82287275801926	0.05	10
Sample F	0.989762788979733	14.8313003950098	0.05	15

5. Conclusions

In this paper, conjugate gradient parameter estimation inverse analysis is employed to determine the parameters of time-lag and fractionality in the fractional non-Fourier heat conduction model for two different skin tissue cases. The finite volume and difference numerical methods are used for solving the direct and sensitivity problems of test cases 1 and 2, respectively. The results show the ability and precision of the CGIM analysis for parameter estimation in the FSPL heat conduction model. This investigation also expresses that the CGIM analysis can be successfully applied for the parameter estimation of the fractional heat equation. Moreover, it is concluded that the CGIM application can be expanded for parameter estimation in fractional calculus.

Author Contributions: Conceptualization, P.G. and S.A.M.M.; methodology, P.G., S.A.M.M., A.A.; software, P.G.; validation, P.G., A.A. and S.A.M.M.; investigation, P.G., A.A., S.A.M.M., M.G. and M.A.S.; data curation, P.G.; writing—original draft preparation, P.G., S.A.M.M., M.G.; writing—review and editing, A.A., M.G. and M.A.S.; supervision, S.A.M.M. and M.A.S. All authors have read and agreed to the published version of the manuscript.

Funding: This research received no external funding.

Institutional Review Board Statement: Not applicable.

Informed Consent Statement: Not applicable.

Data Availability Statement: All data are presented in the present paper.

Acknowledgments: The authors extend their appreciation to the Deanship of Scientific Research at King Khalid University, Abha, Saudi Arabia for funding this work through the Research Group under grant number (R.G.P.1/329/42).

Conflicts of Interest: The authors declare no conflict of interest.

Nomenclature

Latin symbols

c	tissue heat capacity, $Jkg^{-1}\ K^{-1}$
c_b	blood heat capacity $Jkg^{-1}\ K^{-1}$
D	coefficient of thermal diffusion $WJ^{-1}\ m^{-3}$
D_t^{α}	time derivative order
$f(t)$	continuous function
h	skin thickness (mm)
$J_{q\,\alpha}$	sensitivity coefficient of heat respect to order of fractionality
J_{q_τ}	sensitivity coefficient of heat respect to time lag
J_α	sensitivity coefficient respect to order of fractionality
J_τ	sensitivity coefficient respect to time lag
k	tissue thermal conductivity, $Wm^{-1}\ K^{-1}$
m	number of iterations
P	unknown parameters in inverse problem
q_{gen}	generated heat in tissue, Wm^{-3}
q_{met}	metabolic heating source, Wm^{-3}
Q_{in}	laser intensity, Wcm^{-2}
R_d	diffusion reflection
t	time, s
t_f	time duration from the onset to the end, s
t_τ	time period of laser radiation on the skin, s
$u(t)$	unit step function
w_b	blood perfusion rate, m^3m^{-3} tissue
w_j	average of weighted arithmetic
w_r	weight function

Greek symbols

α	order of fractional derivative
α_0	initial guess for order of fractional derivative
ε	error tolerance
θ	temperature of tissue, °C
θ_0	initial temperature, °C
θ_b	blood temperature, °C
θ_c	calculated temperature, °C
θ_{DPL}	measured temperature, °C
ρ	density of tissue, kgm^{-3}
ρ_b	blood density, kgm^{-3}
Γ	gamma function
τ	time lag
τ_T	temperature gradient time lag
τ_q	heat flux time lag
τ_0	initial guess for time lag

Abbreviations

ACGM	Adjoint Conjugate Gradient Method
CGIM	Conjugate Gradient inverse Method
DF	Dermic-Fat interface
DPL	Dual Phase Lag
ED	Epidermis-Dermic interface
FSPL	Fractional Single-Phase Lag
SPL	Single Phase Lag

Appendix A

In Equations (9) and (10), the derivative of the fractional operator relative to α should be obtained. For this purpose, applying the Caputo fractional operator definition leads to a relatively complex analytical relationship that requires the use of a numerical approximation to replace the fractional-order sensitivity coefficients. Therefore, we have:

$$\begin{gathered}\frac{\partial}{\partial\alpha}\left(\frac{\partial^{\alpha}\theta}{\partial t^{\alpha}}\right)=\frac{\partial\sigma_{\alpha}}{\partial\alpha}\sum_{j=1}^{n}\mathrm{w}_{j}^{\alpha}\left(\theta_{i}^{n-j+1}-\theta_{i}^{n-j}\right)\\+\sigma_{\alpha}\sum_{j=1}^{n}\frac{\partial\mathrm{w}_{j}^{\alpha}}{\partial\alpha}\left(\theta_{i}^{n-j+1}-\theta_{i}^{n-j}\right)+\sigma_{\alpha}\sum_{j=1}^{n}\mathrm{w}_{j}^{\alpha}\frac{\partial}{\partial\alpha}\left(\theta_{i}^{n-j+1}-\theta_{i}^{n-j}\right)\end{gathered}\tag{A1}$$

$$\begin{gathered}\frac{\partial}{\partial\alpha}\left(\frac{\partial^{1+\alpha}\theta}{\partial t^{1+\alpha}}\right)=\frac{\partial\sigma_{1+\alpha}}{\partial\alpha}\sum_{j=1}^{n}\mathrm{w}_{j}^{1+\alpha}\left(-2\theta_{i}^{n-j}+\theta_{i}^{n-j+1}+\theta_{i}^{n-j-1}\right)\\+\sigma_{1+\alpha}\sum_{j=1}^{n}\frac{\partial\mathrm{w}_{j}^{1+\alpha}}{\partial\alpha}\left(-2\theta_{i}^{n-j}+\theta_{i}^{n-j+1}+\theta_{i}^{n-j-1}\right)+\sigma_{1+\alpha}\sum_{j=1}^{n}\mathrm{w}_{j}^{1+\alpha}\frac{\partial}{\partial\alpha}\left(-2\theta_{i}^{n-j}+\theta_{i}^{n-j+1}+\theta_{i}^{n-j-1}\right)\end{gathered}\tag{A2}$$

$$\begin{gathered}\frac{\partial\sigma_{1+\alpha}}{\partial\alpha}=\sigma_{1+\alpha}\left[\frac{-\frac{\partial\Gamma(1-\alpha)}{\partial\alpha}}{\Gamma(1-\alpha)}+\frac{1}{1-\alpha}-\ln(\Delta t)\right]\\\frac{\partial\sigma_{\alpha}}{\partial\alpha}=\sigma_{\alpha}\left[\frac{-\frac{\partial\Gamma(1-\alpha)}{\partial\alpha}}{\Gamma(1-\alpha)}+\frac{1}{1-\alpha}-\ln(\Delta t)\right]\\\frac{\partial\Gamma(1-\alpha)}{\partial\alpha}=-\Psi(1-\alpha)\,\Gamma(1-\alpha)\end{gathered}\tag{A3}$$

$$\frac{\partial\mathrm{w}_{j}^{1+\alpha}}{\partial\alpha}=\frac{\partial w_{j}^{\alpha}}{\partial\alpha}=(j-1)^{1-\alpha}\,\ln(j-1)-j^{1-\alpha}\,\ln(j)\tag{A4}$$

Appendix B

The finite volume approach is employed to discretize the controlling equations. The discretization of the sensitivity equation for τ, discussed in [23] in detail, can be obtained as the following:

$$\begin{aligned}
&a_P J_{q_{\tau P}}^{t+\Delta t} = a_E J_{q_{\tau E}}^{t+\Delta t} + a_W J_{q_{\tau W}}^{t+\Delta t} + b \\
&a_E = D\frac{\Delta t}{\Delta x} \quad , \quad a_W = D\frac{\Delta t}{\Delta x} \\
&a_P = a_E + a_W + \Delta x + \Delta x\, {\tau_q}^{\alpha}\sigma_\alpha \\
&b = \left[\Delta x + 2\Delta x\, {\tau_q}^{\alpha}\sigma_\alpha\right] J_{q_{\tau P}}^{t} - \Delta x\, {\tau_q}^{\alpha}\sigma_\alpha J_{q_{\tau P}}^{t-\Delta t} + \Delta x\, D\, w_b\rho_b c_b \frac{J_{\tau_E}^{t} - J_{\tau_W}^{t}}{2} \\
&\quad -\Delta x\, {\tau_q}^{\alpha}\sigma_\alpha\, [\text{source 1} - \text{source 2}] \\
&\quad -\Delta x\, {\tau_q}^{\alpha-1}\sigma_\alpha [\text{source 3} - \text{source 4}]
\end{aligned} \tag{A5}$$

where

$$\begin{aligned}
\text{source 1} &= \sum_{j=2}^{t+\Delta t} \mathrm{w}_j^{\alpha}\left(J_{q_{\tau P}}^{t-j+\Delta t-1} - J_{q_{\tau P}}^{t-j+\Delta t}\right) \\
\text{source 2} &= \sum_{j=2}^{t} \mathrm{w}_j^{\alpha}\left(J_{q_{\tau P}}^{t-j-1} - J_{q_{\tau P}}^{t-j}\right) \\
\text{source 3} &= \sum_{j=1}^{t+\Delta t} \mathrm{w}_j^{\alpha}\left(q_P^{t-j+\Delta t+1} - q_P^{t-j+\Delta t}\right) \\
\text{source 4} &= \sum_{j=1}^{t} \mathrm{w}_j^{\alpha}\left(q_P^{t-j+1} - q_P^{t-j}\right)
\end{aligned} \tag{A6}$$

where w is the weighted arithmetic mean [27],

$$\begin{aligned}
\sigma_\alpha &= \frac{1}{\Gamma(2-\alpha)} \cdot \frac{1}{2-\alpha} \cdot \frac{1}{\Delta t^{\alpha}} \\
\mathrm{w}_j^{\alpha} &= \left(j^{2-\alpha} - (j-1)^{2-\alpha}\right)
\end{aligned} \tag{A7}$$

the sensitivity of temperature, i.e., J_τ, is reached as the following:

$$J_{\tau P}^{t+\Delta t} = J_{\tau P}^{t} + \frac{\Delta t}{\rho c}\left[-\frac{J_{q_\tau E}^{t+\Delta t} - J_{q_\tau W}^{t+\Delta t}}{2\Delta x} - w_b\rho_b c_b J_{\tau P}^{t}\right] \tag{A8}$$

The discretization of the sensitivity equation for α is also obtained as the following:

$$\begin{aligned}
&a_P J_{q_{\alpha P}}^{t+\Delta t} = a_E J_{q_{\alpha E}}^{t+\Delta t} + a_W J_{q_{\alpha W}}^{t+\Delta t} + b \\
&a_E = D\frac{\Delta t}{\Delta x} \quad , \quad a_W = D\frac{\Delta t}{\Delta x} \\
&a_P = a_E + a_W + \Delta x + \Delta x\, {\tau_q}^{\alpha}\sigma_{1+\alpha} \\
&b = \left[\Delta x + 3\Delta x\, {\tau_q}^{\alpha}\sigma_{1+\alpha}\right] J_{q_P}^{t} - 3\Delta x\, {\tau_q}^{\alpha}\sigma_{1+\alpha} J_{q_P}^{t-\Delta t} + 3\Delta x\, {\tau_q}^{\alpha}\sigma_{1+\alpha} J_{q_P}^{t-2\Delta t} \\
&\quad +\Delta x\, D\, w_b\rho_b c_b \frac{J_{\tau_E}^{t} - J_{\tau_W}^{t}}{2} + \Delta x\, {\tau_q}^{\alpha}\, \sigma_\alpha \ln\tau\, [\text{source 2} - \text{source 1}] \\
&\quad +\Delta x\, {\tau_q}^{\alpha}\frac{\partial\sigma_{1+\alpha}}{\partial\alpha}[\text{source 4} - \text{source 3}] + \Delta x\, {\tau_q}^{\alpha}\sigma_{1+\alpha}[\text{source 6} - \text{source 5}] \\
&\quad +\Delta x\, {\tau_q}^{\alpha}\sigma_{1+\alpha}[\text{source 8} - \text{source 7}]
\end{aligned} \tag{A9}$$

where

$$\begin{aligned}
\text{source 1} &= \sum_{j=1}^{t+\Delta t} w_j^{\alpha}\left(q_P^{t-j+\Delta t+1} - q_P^{t-j+\Delta t}\right)\\
\text{source 2} &= \sum_{j=1}^{t} w_j^{\alpha}\left(q_P^{t-j+1} - q_P^{t-j}\right)\\
\text{source 3} &= \sum_{j=2}^{t+\Delta t} w_j^{1+\alpha}\left(q_P^{t+\Delta t-j+1} - 2q_P^{t+\Delta t-j} + q_P^{t+\Delta t-j-1}\right)\\
\text{source 4} &= \sum_{j=2}^{t} w_j^{1+\alpha}\left(q_P^{t-j+1} - 2q_P^{t-j} + q_P^{t-j-1}\right)\\
\text{source 5} &= \sum_{j=1}^{t+\Delta t} \frac{\partial w_j^{1+\alpha}}{\partial \alpha}\left(q_P^{t+\Delta t-j+1} - 2q_P^{t+\Delta t-j} + q_P^{t+\Delta t-j-1}\right)\\
\text{source 6} &= \sum_{j=1}^{t} \frac{\partial w_j^{1+\alpha}}{\partial \alpha}\left(q_P^{t-j+1} - 2q_P^{t-j} + q_P^{t-j-1}\right)\\
\text{source 7} &= \sum_{j=2}^{t+\Delta t} w_j^{1+\alpha}\left(J_{q_{\alpha P}}^{t-j+\Delta t+1} - 2J_{q_{\alpha P}}^{t-j+\Delta t} + J_{q_{\alpha P}}^{t-j+\Delta t-1}\right)\\
\text{source 8} &= \sum_{j=2}^{t} w_j^{1+\alpha}\left(J_{q_{\alpha P}}^{t-j+1} - 2J_{q_{\alpha P}}^{t-j} + J_{q_{\alpha P}}^{t-j-1}\right)
\end{aligned} \tag{A10}$$

where w is the weighted arithmetic mean [27],

$$\begin{aligned}
\sigma_{1+\alpha} &= \tfrac{1}{\Gamma(1-\alpha)} \cdot \tfrac{1}{1-\alpha} \cdot \tfrac{1}{\Delta t^{1+\alpha}}\\
\mathrm{w}_j^{1+\alpha} &= \left(j^{1-\alpha} - (j-1)^{1-\alpha}\right)
\end{aligned} \tag{A11}$$

Finally, the temperature sensitivity with respect to α, i.e., J_{α}, is obtained as follows:

$$J_{\alpha P}^{\,t+\Delta t} = J_{\alpha P}^{\,t} + \frac{\Delta t}{\rho c}\left[-\frac{J_{q_{\alpha E}}^{\,t+\Delta t} - J_{q_{\alpha W}}^{\,t+\Delta t}}{2\Delta x} - w_b \rho_b c_b J_{\alpha P}^{\,t}\right] \tag{A12}$$

References

1. Tang, D.W.; Araki, N. Non-fourier heat conduction behavior in finite mediums under pulse surface heating. *Mater. Sci. Eng. A* **2000**, *292*, 173–178. [CrossRef]
2. Hsu, P.T.; Chu, Y.H. An inverse non-fourier heat conduction problem approach for estimating the boundary condition in electronic device. *Appl. Math. Model.* **2004**, *28*, 639–652. [CrossRef]
3. Yang, C.Y. Direct and inverse solutions of the hyperbolic heat conduction problems. *J. Thermophys. Heat Transf.* **2005**, *19*, 217–225. [CrossRef]
4. Hsu, P.T. Estimating the boundary condition in a 3D inverse hyperbolic heat conduction problem. *Appl. Math. Comput.* **2006**, *177*, 453–464. [CrossRef]
5. Krishna, M.V.; Chamkha, A.J. Hall and ion slip effects on magnetohydrodynamic convective rotating flow of Jeffreys fluid over an impulsively moving vertical plate embedded in a saturated porous medium with ramped wall temperature. *Numer. Methods Partial. Differ. Equ.* **2021**, *37*, 2150–2177. [CrossRef]
6. Hussain, S.; Ismael, M.A.; Chamkha, A.J. Impinging jet into an open trapezoidal cavity partially filled with a porous layer. *Int. Commun. Heat Mass Transf.* **2020**, *118*, 104870. [CrossRef]
7. Kumar, B.; Seth, G.; Singh, M.; Chamkha, A. Carbon nanotubes (CNTs)-based flow between two spinning discs with porous medium, Cattaneo–Christov (non-fourier) model and convective thermal condition. *J. Therm. Anal. Calorim.* **2021**, *146*, 241–252. [CrossRef]
8. Kumar, K.G.; Reddy, M.G.; Sudharani, M.; Shehzad, S.; Chamkha, A.J. Cattaneo–Christov heat diffusion phenomenon in Reiner–Philippoff fluid through a transverse magnetic field. *Phys. A* **2020**, *541*, 123330. [CrossRef]
9. Kotha, G.; Kolipaula, V.R.; Rao, M.V.S.; Penki, S.; Chamkha, A.J. Internal heat generation on bioconvection of an MHD nanofluid flow due to gyrotactic microorganisms. *Eur. Phys. J. Plus* **2020**, *135*, 1–19. [CrossRef]
10. Chamkha, A.J.; Nabwey, H.A.; Abdelrahman, Z.; Rashad, A. Mixed bioconvective flow over a wedge in porous media drenched with a nanofluid. *J. Nanofluids* **2019**, *8*, 1692–1703. [CrossRef]
11. Sheremet, M.A.; Pop, I. Thermo-bioconvection in a square porous cavity filled by oxytactic microorganisms. *Transp. Porous Media* **2014**, *103*, 191–205. [CrossRef]
12. Liu, K.C.; Lin, C.T. Solution of an inverse heat conduction problem in a bi-layered spherical tissue. *Numer. Heat Transf. A* **2010**, *58*, 802–818. [CrossRef]

13. Azimi, A.; Ahmadikia, A.; Masouleh, K.B. Base temperature estimation of non-fourier fin with different profiles by the use of inverse analysis. *J. Appl. Math. Modeling* **2009**, *33*, 2907–2918.
14. Das, R.; Mishra, S.C.; Kumar, T.P.; Uppaluri, R. An inverse analysis for parameter estimation applied to a non-fourier conduction–radiation problem. *Heat Transf. Eng.* **2011**, *32*, 455–466. [CrossRef]
15. Ghazizadeh, H.R.; Azimi, A.; Maerefat, M. An inverse problem to estimate relaxation parameter and order of fractionality in fractional single-phase-lag heat equation. *Int. J. Heat Mass Transf.* **2012**, *55*, 2095–2101. [CrossRef]
16. Azimi, A.; Bamdad, K.; Ahmadikia, H. Inverse hyperbolic heat conduction in fins with arbitrary profiles. *Numer. Heat Transf. A* **2012**, *61*, 220–240. [CrossRef]
17. Wu, T.S.; Lee, H.L.; Chang, W.J.; Yang, Y.C. An inverse hyperbolic heat conduction problem in estimating pulse heat flux with a dual-phase-lag model. *Int. Commun. Heat Mass Transf.* **2015**, *60*, 1–8. [CrossRef]
18. Mozafarifard, M.; Azimi, A.; Mehrzad, S. Numerical simulation of dual-phase-lag model and inverse fractional single-phase-lag problem for the non-fourier heat conduction in a straight fin. *J. Therm. Sci.* **2020**, *29*, 632–646. [CrossRef]
19. Ali, M.; Aziz, S.; Malik, S.A. Inverse source problems for a space–time fractional differential equation. *Inverse Probl. Sci. Eng.* **2020**, *28*, 47–68. [CrossRef]
20. Cheng, X.; Yuan, L.; Liang, K. Inverse source problem for a distributed-order time fractional diffusion equation. *J. Inverse Ill-Posed Probl.* **2020**, *28*, 17–32. [CrossRef]
21. Sun, C.; Liu, J. An inverse source problem for distributed order time-fractional diffusion equation. *Inverse Probl.* **2020**, *36*, 055008. [CrossRef]
22. Tuan, N.H.; Zhou, Y.; Can, N.H. Identifying inverse source for fractional diffusion equation with Riemann–Liouville derivative. *Comput. Appl. Math.* **2020**, *39*, 75. [CrossRef]
23. Goudarzi, P.; Azimi, A. Numerical simulation of fractional non-fourier heat conduction in skin tissue. *J. Therm. Biol.* **2019**, *84*, 274–284. [CrossRef]
24. Ozisik, M.N.; Orlande, H.; Kassab, A. Inverse heat transfer: Fundamentals and Applications. *Appl. Mech. Rev.* **2002**, *55*, B18–B19. [CrossRef]
25. Liu, K.C.; Cheng, P.J.; Wang, Y.N. Analysis of non-fourier thermal behavior for multi-layer skin model. *Therm. Sci.* **2011**, *15*, 61–67. [CrossRef]
26. Zhou, J.; Chen, J.; Zhang, Y. Dual-phase lag effects on thermal damage to biological tissues caused by laser irradiation. *Comput. Biol. Med.* **2009**, *39*, 286–293. [CrossRef] [PubMed]
27. Ghazizadeh, H.; Maerefat, M.; Azimi, A. Explicit and implicit finite difference schemes for fractional Cattaneo equation. *J. Comput. Phys.* **2010**, *229*, 7042–7057. [CrossRef]